SAND2022-5622C

The 10th International Conference on Modeling and Diagnostics for Advanced Engine Systems (COMODIA 2022), July 5-8, 2022, Sapporo, Japan

0094

Influence of Nitric Oxide and Other Factors on Acoustic Knock Onset for Lean DISI Engine Operation

Magnus Sjöberg and Namho Kim
Sandia National Laboratories
PO Box 969, Livermore, CA 94551, USA

Naoyoshi Matsubara, Nozomi Yokoo and Koichi Nakata
Toyota Motor Corporation, Japan

Keywords: Lean SI Combustion, Knock Generation, SI Engine Fuel Effects

ABSTRACT

Spark-ignition (SI) engine efficiency can be increased by operating lean and with increased compression ratio (CR), but both of these measures tend to increase the propensity for undesirable acoustic knock generation. It is well known that increased CR makes the engine more prone to knock due to increased combustion pressures and temperatures, but it may be less well understood why lean operation would exacerbate knock generation. For typical gasoline-range fuels, the laminar flame speed becomes very low (roughly only 20% compared to stoichiometric conditions) for an air-excess ratio (λ) of 2. Indirectly, this exacerbates the knock challenge in two ways; a) it may necessitate operation with a combustion phasing near Top Dead Center (TDC) to complete the combustion before expansion cooling occurs, b) it increases cycle-to-cycle variations, making it more challenging to operate near the knock limits. In addition, the high intake pressure required for lean operation (nearly a factor of two higher for $\lambda = 2$ compared to $\lambda = 1$) increases the oxygen concentration which promotes end-gas autoignition and knock generation.

Towards overcoming these challenges of lean combustion, this study aims to provide a better understanding of fuel autoignition under various conditions. First, to reveal the octane appetite under lean conditions, this experimental work utilized fuels of varying Research Octane Number (RON) and octane sensitivity (S). It was found that lean operation favored fuels that have high RON and high S since those were less knock limited. However, two compositionally different fuels with similarly high RON and S exhibited notable difference in knock limits under lean operation, indicating that RON and S may fail to accurately rank order fuels' knock propensity. Second, the experiments show that under boosted conditions end-gas autoignition becomes sensitive to the level of trapped residual nitric oxide (NO), which in turn is very sensitive to variations of both actual λ and combustion phasing, among other factors. The results suggest that strong knock-suppression benefits could be realized if single-ppm NO mole fraction can be consistently maintained in the reactants. Finally, it is noted that maintaining knock-free operation is particularly important for lean operation because the lower peak combustion temperatures lower the speed of sound, which in turn shifts the frequency content of the in-cylinder knock to a lower frequency range. Lower knock frequencies can increase the transmission efficiency from the combustion chamber to the outer surfaces of the engine, potentially increasing engine noise levels if knock occurs.

INTRODUCTION

At the recent Glasgow Climate Change Conference, a majority of the world's countries have officially recognized that emissions of green-house gases (GHG) must be reduced drastically over the coming decades [1]. For personal transportation, increased electrification is an important long-term technical solution to reduced GHG emissions. However, full battery-electric vehicles (BEV) may not be the optimal solution for all applications and markets, especially until charging infrastructure has been fully developed. Hence, there is a need to further develop internal combustion engines to achieve higher thermal efficiency and less GHG emissions per driven distance. At the same time, to support transportation sectors that are difficult to electrify, there is an increased need to develop alternative fuels that are based on non-petroleum sources. This creates an opportunity to develop a new gasoline-type fuel that enables both higher engine and system efficiencies, as well as much lower GHG emissions. It has been well established that onset of engine knock limits the efficiency of SI engines [2]. For fuels used in the automotive market, RON and/or motor octane number (MON) are used to specify a fuel's anti-knock quality [3,4]. In the US and some other countries, the fuels are marketed based on their anti-knock index (AKI), which is the average of the RON and MON values.

$$AKI = (RON + MON) / 2 \quad (1)$$

Historic data from the US market show the benefit of fuels with increased AKI in enabling higher CR and increased transportation efficiency [5]. Technically, the use of AKI made sense when the engines were less refined and operated hotter. However, advances in SI engine technology has rendered AKI less relevant as a metric for

a fuel's anti-knock quality [6]. Instead, there is growing consensus that RON in combination with octane sensitivity (S) is a more relevant metric for a fuel's anti-knock performance in modern SI engines. S is defined as the difference between RON and MON.

$$S = RON - MON \quad (2)$$

For a boosted SI engine that operates with stoichiometric combustion and relatively cool combustion-chamber surfaces, both increased RON and increased S of the fuel provide knock-suppression benefits [7,8]. However, when considering future lean-burn engines, it is not clear if RON and S are adequate anti-knock metrics. This study aims at contributing to this needed understanding. Furthermore, this study aims at demonstrating why knock limits are closely related to the performance of a lean-burn engine. In this context, the important role of retained NO will be highlighted. Finally, it will be demonstrated how lean operation affects the frequency content of the acoustic knock.

EXPERIMENTAL SETUP

The engine used for these experiments is a single-cylinder four-valve research engine that was set up in an all-metal configuration for performance testing. Both a continuously fired mode and a skip-fired mode were used. For these tests, triple injections during the intake stroke were used to generate a relatively well-mixed charge, and the fuel-injection pressure was maintained at 120 bar. The piston has a moderately deep piston bowl to aid the stratification of fuel, as illustrated in Fig. 1. This feature was utilized to enrich the area near the spark plug using a small pilot injection at the time of spark for all operation with a background $\lambda = 2$, supplied by the early injections.

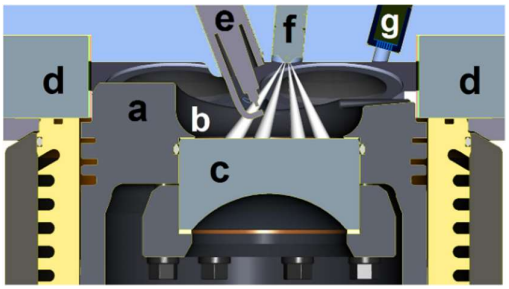

Figure 1. Cross-section of combustion chamber at TDC: a - piston, b - piston bowl, c - piston-bowl window, d - pent-roof windows, e - spark plug, f - fuel injector, and g - pressure sensor with flame arrestor. Aluminum (d) and Invar (c) window blanks were used in this study.

Engine specifications are given in Table 1. For all data, the phasings of the cam shafts relative to the crank shaft were maintained constant and set to provide both low residual levels and high volumetric efficiency [9]. Regarding intake flows, the engine was operated in two different configurations, as indicated by Table 1. In one configuration, both intake valves were active, and this generated a low-tumble in-cylinder flow without swirl. In the other configuration, one intake valve was deactivated which created a swirling flow with higher tumble level. The higher tumble is presumably caused by a doubling of the intake-flow speeds associated with a strong reduction of the flow area.

Table 1 Engine specifications.

Displacement	0.552 liters
Bore	86.0 mm
Stroke	95.1 mm
Connecting rod length	166.7 mm
Geometric compression ratio	12:1
Intake valve diameter	35.1 mm
Intake valve angle relative cylinder axis	18°
Exhaust valve diameter	30.1 mm
Exhaust valve angle relative cylinder axis	16°
Swirl / tumble indexes	
One intake valve deactivated	2.7 / 0.62
Two intake valves activate	0.0 / 0.27
Fuel injector	Bosch 8-hole solenoid-type
Hole orientation	Symmetric with 60° included angle
Hole size	Stepped-hole, min. dia. = 0.125 mm

Sonic-flow nozzles were used to meter air and nitrogen into the intake system. In addition, for NO-seeding experiments, a mass-flow controller (sometimes in combination with a fixed nozzle for higher flow rates) was used to meter a mixture of 5% NO in N_2 into the intake air stream, following Ref. [10].

Experimental Procedure and Data Analysis

For each operating point, the engine was allowed to run for several minutes until all measured parameters were stable, at which point data were acquired. Fuel-flow rate and thermocouple readouts were averaged over roughly one minute.

For continuously fired operation, 500 consecutive cycles were recorded, including the in-cylinder pressure, spark current, intake and exhaust pressure, and fuel pressure using 0.1°CA resolution. For the in-cylinder pressure, an uncooled Kistler 6125C piezoelectric sensor was used in combination with a Kistler 5010B charge amplifier. The pressure sensor was mounted in a hole located between the fuel injector and a side window, as indicated in Fig. 1g. To avoid thermal shock, a flame arrestor was mounted between the sensor and the combustion chamber. The vertical distance from the tip of the sensor and the combustion chamber was roughly 5 mm, and the entry hole had a diameter of 4 mm.

The apparent heat-release rate (AHRR) was computed from the in-cylinder pressure for each individual cycle using a constant ratio of specific heats ($\gamma = 1.33$ for stoichiometric and $\gamma = 1.36$ for lean operation) following Ref. [2]. For computing combustion-phasing metrics like the 50% burn point (CA50), the AHRR was integrated from spark timing (ST) until AHRR reaches zero at the end of the combustion event. For operation with knock, even moderate pressure oscillations can make the resulting AHRR traces oscillate strongly. To facilitate the interpretation of the AHRR traces, a digital FFT-based low-pass filter was applied, as illustrated in Fig. 3 of Ref.

[11]. The filter maintains all energy below 1.5 kHz, and has a gradual roll-off above this frequency.

For determining the level of knock, the same metric developed in Ref. [11] named Knock Intensity (KI) is used. In short, first a high-pass filtered pressure trace (with 0.1°CA resolution) was computed for each individual cycle in the 0-80°CA range by subtracting the low-pass filtered pressure from the raw pressure. Subsequently, the frequency content of this high-pass filtered pressure was computed. To quantify the knock level, KI is defined as the sum of all data points in the 4.5 – 28 kHz range for each individual cycle. The frequency range for KI computation changed from that introduced in Ref. [11] based on the experimental results for $\lambda = 2$ operation, which will be explained in more detail. For computing an average KI for a specific operating point, KI of each of the 500 cycles was then averaged.

To provide an alternate measure of acoustic knock, an accelerometer (Wilcoxon Research Model 799M) was installed on top of the cylinder-head assembly. (For visualization, the reader is referred to Fig. 12b in Ref. [9].) The frequency content of the accelerometer was computed identically to that of the in-cylinder pressure, focusing on the 0-80°CA range and rejecting all content below 1.5 kHz.

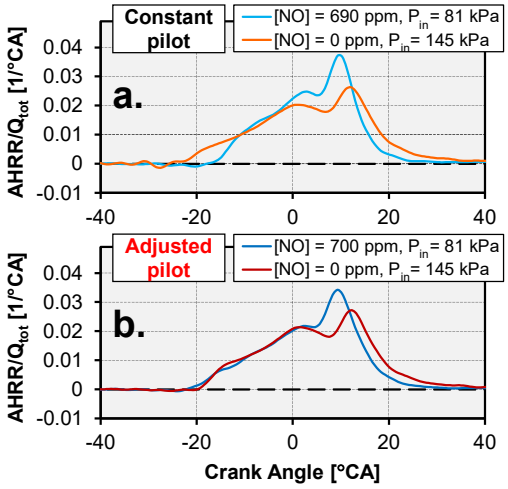

Fig. 2 Adjustment of pilot amount with [NO] and P_{in} to achieve consistent deflagration-based AHRR.

As mentioned above, to stabilize ultra-lean operation, a small pilot injection was employed at the time of spark. The timing of the pilot injection was such that the head of the two penetrating pilot fuel jets next to the spark-plug electrode passed by the spark-plug gap roughly 1°CA before the beginning of the spark discharge. (The reader is referred to Ref. [12] for visualization of similar conditions.) Initially, a fixed pilot injection duration was employed. However, such a strategy meant that the relative amount of enrichment near the spark plug changed with the intake pressure (P_{in}), causing the deflagration-based AHRR to vary between conditions, as exemplified in Fig. 2a. Hence, a new strategy was devised whereby the pilot amount was adjusted for each P_{in} to maintain the dwell between spark timing and the 10% burn point (CA10) nearly constant around 17°CA. As a result, the normalized AHRR profiles remain much more similar during the main deflagration phase (-18 to 2°CA), as shown in Fig. 2b. This strategy required the electrical command duration to be adjusted in the range of 209 to 240 µs, corresponding to 0.85 to 2.44 mg of fuel per pilot injection. For the lean results below with $\lambda = 2$ in the end-gas, the pilot injection fuel mass was not included in the computation of λ or fuel/air-equivalence ratio ($\phi_{end\text{-}gas}$).

Fuels

This study is concerned with the influence of octane ratings and fuel composition on knock limits and autoignition for operation with $\lambda = 2$. Four different fuels were used, and selected specifications are presented in Table 2. To examine the role of autoignition reactivity on lean knock, RON and S were varied substantially. The fuels have been given names that represent their respective compositions. Specifically, the fuel named High Olefins has a relatively high fraction of unsaturated hydrocarbons (*i.e.* alkenes / olefins). Similarly, the High Cycloalkane fuel contains a relatively high level of cyclic hydrocarbons (*i.e.* cycloalkanes / naphthenes). These two fuels both have high RON and high S, offering an opportunity to examine the relevance of RON and S under lean conditions for two fuels with differing compositions.

Table 2. Selected fuel properties and ratings for the four fuels used in this study. Data from SwRI and NREL [13].

	E10 Gasoline (RD5-87)	iso-Octane	High Olefins (HO)	High Cyclo-alkanes (HCA)
RON	92.1	100	98.3	97.8
MON	84.8	100	87.9	86.9
Octane Sensitivity	7.3	0	10.4	11.0
Oxygenates [vol.%]	10.6	0	0	0
Aromatics [vol.%]	20.9	0	13.4	33.2
Alkanes [vol.%]	49.4	100	56.4	40.6
Cycloalkanes [vol.%]	11.3	0	2.9	24.2
Olefins [vol.%]	4.9	0	26.5	1.6
T10 [°C]	57	-	77	56
T50 [°C]	98	99	104	87
T90 [°C]	156	-	136	143
Heat of Combustion [MJ/kg]	41.9	44.3	44.1	43.2
Heat of Vaporization [kJ/kg]	412	271	333	393
AFR Stoichiometric	14.1	15.1	14.8	14.5
Particulate Matter Index	1.68	0.19	1.00	1.49

RESULTS AND DISCUSSION

Highly Knock Limited Operation - Three Fuels

For these initial tests, the engine was operated with only one intake valve, consistent with previous knock studies, *e.g.* [8,10]. The operating conditions of these continuously fired experiments are listed in Table 3.

The engine speed was maintained constant at 1400 rpm for all data and no N_2 dilution was used for these tests. For each fuel, knock-limited stoichiometric operation was first established with a target $IMEP_g$ of 800 kPa, requiring $P_{in} \approx 80$ kPa. Based on this operation, a lean operating point with $\phi_{end\text{-}gas} = 0.5$, was established by maintaining

the same amount of fuel injected during the intake stroke, but with a doubled amount of intake-air flow. As shown in Fig. 3c, this increased P_{in} by roughly 85% to ≈150 kPa.

Table 3. Continuously fired highly knock-limited operating conditions.

Engine Speed	1400 rpm
Mode	Continuously Fired
$\phi_{end\text{-}gas}$	1.0 / 0.5 (excluding pilot for lean)
$IMEP_g$	≈ 8 bar for ϕ = 1.0
Intake Pressure, ϕ = 1.0	78 - 82 kPa
Intake Pressure, ϕ = 0.5	145 - 152 kPa
Injection Pressure	120 bar
Start of First Injection	-310°CA
# of Fuel Injections	3 early (+ 1 pilot for lean)
ΔCA between SOIs of Early Fuel Injections	14°CA
Spark Energy	106 mJ
Spark Timing Criterion	KI = 50 - 80 kPa
Coolant Temperature	75°C
Intake Temperature	43°C

All three fuels were operated at the knock limit for both the stoichiometric and lean points. As Fig. 3a shows, the fuels have different stoichiometric knock limits, as expected based on the greatly varying RON and S. The E10 RD5-87 fuel with RON = 92 is the most knock limited fuel for both stoichiometric and lean operation. It is interesting that iso-octane becomes substantially more knock limited for lean operation, while the High-Olefin fuel becomes substantially less knock limited when $\phi_{end\text{-}gas}$ is reduced from 1.0 to 0.5. This observation will be revisited after K values have been computed. Figure 4 presents octane-index (OI) regression analysis of the current data, following [14] and defining OI as:

$$OI = RON - K \cdot S \quad (3)$$

It shows that the combined effect of lean operation and increased P_{in} shifts the K value from near zero to -0.54, explaining why the KL-CA50 trends for iso-octane and High-Olefin fuels cross in Fig. 3a. A negative K value means that a fuel with higher S will provide knock-suppression benefits. Vuilleumier *et al.* [8] showed that for stoichiometric operation, the knock limits of fuels with high octane sensitivity were less affected by increased P_{in}, especially for operation with K < 1, corresponding to "beyond-RON". Those observations appear to hold also for these lean conditions. Furthermore, Mittal and Heywood showed that K becomes increasingly negative for both lean operation and with increased intake pressure, consistent with the current results [15].

To ensure thermal efficiency gains from lean operation, it is important to maintain a 10-90% burn duration of 30°CA or less [16,17]. Figure 3b shows that for $\phi_{end\text{-}gas}$ = 0.5, all three fuels have burn durations that exceed 30°CA. Interestingly, the High-Olefin fuel has the most advanced KL-CA50, and it also has the shortest burn duration. This highlights the need to phase the combustion closer to TDC for lean operation, which benefits the combustion rate for a lean charge due to higher turbulence [18] and higher reactant temperatures (which stem of the higher peak pressures that result from an earlier combustion phasing). Kaneko *et al.* [19] also noted the benefits of more knock-resistant fuels for operation with $\phi_{end\text{-}gas}$ = 0.5, allowing earlier combustion phasing and higher thermal efficiency.

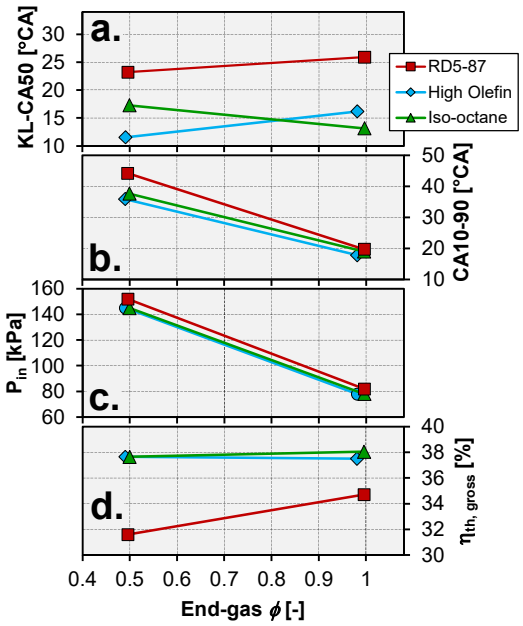

Fig. 3 a) KL-CA50, b) 10-90% burn duration (CA10-90), c) P_{in} and d) gross indicated thermal efficiency ($\eta_{th, gross}$) versus $\phi_{end\text{-}gas}$ for RD5-87, iso-octane, and High-Olefin.

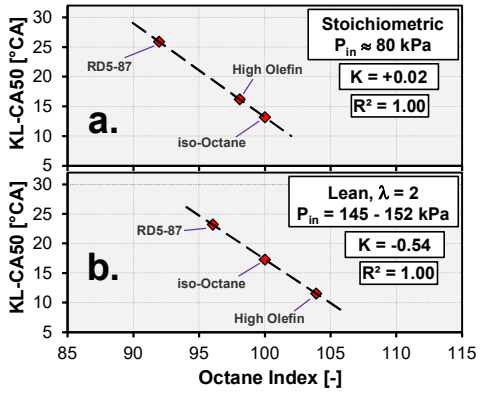

Fig. 4 KL-CA50 vs best-fit Octane Index (OI) for a) stoichiometric and b) lean conditions.

Due to the relatively late KL-CA50 for all three fuels, Fig. 3d shows that no thermal efficiency gain was realized by lean operation in this set of experiments. This highlights the need to manage lean knock limits to fully exploit the efficiency gains offered by lean SI engine operation.

Less Knock Limited Operation - Two Fuels

As discussed in conjunction with Fig. 3, if knock is forcing the combustion phasing to be retarded that may

prevent any efficiency gains from lean operation. To avoid such situation and enable efficiency benefits from lean operation, various steps can be taken to mitigate lean knock, such as; a reduction of CR, reduced engine load, increased knock resistance of the fuel, and a higher engine speed (which reduces time for autoignition). In the following, focus shifts to the two fuels with high RON and S, operated at a slightly lower load compared to the previous section, as specified in Table 4.

Table 4. Reduced load and intake pressure for less knock-limited continuously fired operation (*cf.* Table 3).

IMEPg	≈ 7 bar for ϕ = 1.0
Intake Pressure, ϕ = 1.0	68 - 69 kPa
Intake Pressure, ϕ = 0.5	125 kPa

The lower load reduces knock propensity and allows a more advanced combustion phasing. In addition, for the following data sets both intake valves were active, corresponding to typical production engines. The change from single to dual intake valves further reduced the knock propensity, possibly due to a more uniform flame spread [17]. The observations are summarized in Fig. 5.

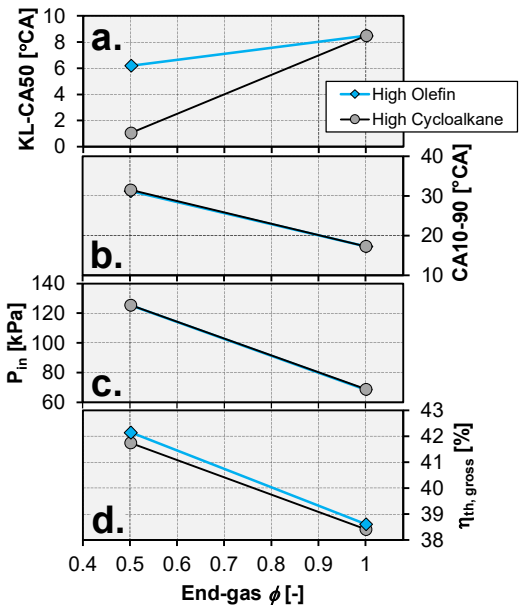

Fig. 5 a) KL-CA50, b) CA10-90, c) P_{in} and d) $\eta_{th,\,gross}$ versus $\phi_{end\text{-}gas}$ for High-Olefin and High-Cycloalkane fuels.

Figure 5a shows that for stoichiometric operation, KL-CA50 is very similar for the two fuels, which is expected based on the very similar RON and S ratings. Figure 6 shows that the AHRR profiles are also very similar for the two fuels under stoichiometric conditions. However, Fig. 5a shows a relatively strong deviation of the lean knock limits, indicating that for lean conditions RON and S become less adequate for rank ordering fuels in terms of knock limits. This observation suggests that new lean SI engine knock fuel property metrics should be considered, similar to recent efforts on lean autoignition fuel rating under HCCI-like conditions [20]. It is not clear why the High-Cycloalkane fuel has a higher knock resistance than the High-Olefin fuel at the lean condition. There are two primary factors to consider. First, the autoignition chemistry of the fuels may respond differently to changes of ϕ, which is reduced by 50% for the lean operation. Differences in "ϕ-sensitivity" between fuels have been observed and exploited in previous work [21]. Second, lean operation results in much higher peak combustion pressures, and it is known that fuels respond differently to changes in pressure [22,23]. Future research should be able to clarify if either of these two factors is responsible for the different trends shown in Fig. 5a. However, there may be a third factor behind the higher lean knock resistance of High-Cycloalkane, namely different sensitivities to changes of the in-cylinder NO mole fraction.

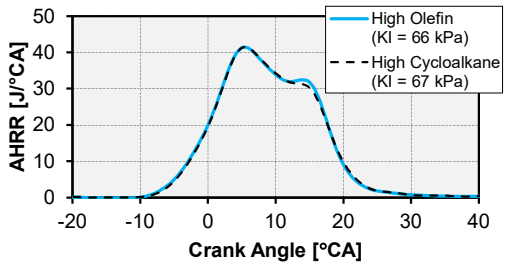

Fig. 6 Comparison of AHRR and knock level for High-Olefin and High Cycloalkane fuels under stoichiometric conditions.

With the operation being less knock limited than that of the previous section, CA50 can be advanced to 6°CA or earlier which benefits lean operation (*cf.* Figs. 3a and 5a). For these lower loads under lean conditions, Fig. 5b shows that the 10-90°CA combustion duration only slightly exceeds the target value of 30°CA. Consequently, Fig. 5d shows a substantial gain of the gross thermal indicated efficiency. However, it is likely that the relative gain of efficiency would have been higher for a fast-burn combustion system that can maintain an even shorter burn duration for every cycle during lean operation [24].

As will be shown in the following, for lean operation under these conditions, cycle-to-cycle variability and the knock limit together hinder optimal engine operation and therefore limit the observed thermal efficiency gain. Figure 7 shows that for lean operation there is significant cycle-to-cycle variability of KI, $IMEP_g$, and combustion duration. Cycles that happen to be more advanced due to somewhat faster early deflagration tend to have shorter burn duration and higher $IMEP_g$, but at the price of increased KI. This highlights the coupling between end-gas autoignition, knock and high thermal efficiency for lean operation with a low-tumble combustion system. Since the tumble level is low, it is hypothesized that the turbulence level tends to be low in the end-gas towards the end of the combustion, slowing the burn-out process. However, when end-gas autoignition takes place, this speeds up the final stages of the combustion even if the turbulence level is low. A total of 500 cycles are plotted in

Fig. 7. Out of those, 188 are highlighted with green symbols, having fast combustion, high IMEP and low KI. This highlights the potential benefits of stable lean combustion and provides motivation for further research.

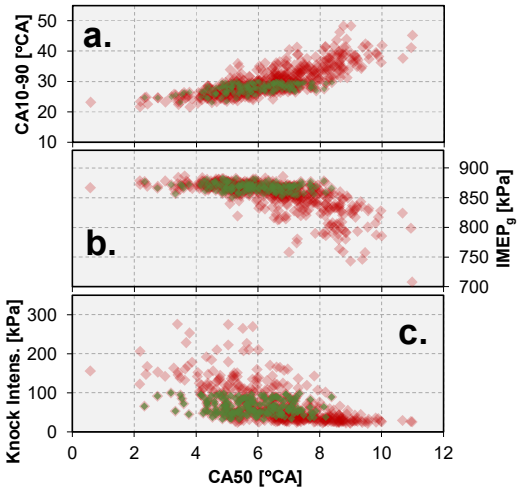

Fig. 7 Natural cycle-to-cycle variations in CA10-90, IMEP$_g$ and KI with respect to CA50 for $\phi_{end\text{-}gas} = 0.50$ with the High-Olefin fuel. Green symbols = ideal cycles

A high-tumble combustion system could potentially sustain fast deflagration throughout the end-gas regions [25], thus acting to decouple knock and high efficiency to some degree. Mahendar *et al.* [26] investigated different piston shapes that could increase turbulence during the burn-out phase. They also noted that the onset of knock can limit the thermal efficiency for a lean-burn SI engine.

Continuously Fired Operation with NO-seeding

Previous research has shown that trace species that are carried from one cycle to the next via residuals or exhaust-gas recirculation (EGR) can strongly influence autoignition. NO has been identified as a particularly important trace species [10,27]. Hence, to determine the role of NO for the observed lean knock limits, additional experiments were carried out. For these experiments, a new operating point with slight N_2 dilution was established, lowering the intake [O_2] from 20.9 to 20.3%. This was done to enable operation with a constant intake [O_2] for the NO seeding experiments. When increasing amounts of NO/N_2 seed gas were introduced, the N_2-only dilution flow was reduced correspondingly (*cf.* Fig. 2 in Ref. [10]). The results of this exercise are shown in Fig. 8.

First, it can be noted that the lowest [NO] level accessed here is 25 ppm, which corresponds to the NO retained with the residuals. Two experimental methods were tested. In Method A the intake flow rates were held constant when the intake [NO] was increased, rendering a nearly constant P_{in}. In this case, the autoignition-promoting effect of NO is clear from Fig. 8a, forcing CA50 retard to maintain a constant KI. However, as discussed above, lean combustion can be very sensitive to CA50 retard. Indeed, Fig. 8b shows elevated CoV of IMEP$_g$ for [NO] > 300 ppm with Method A.

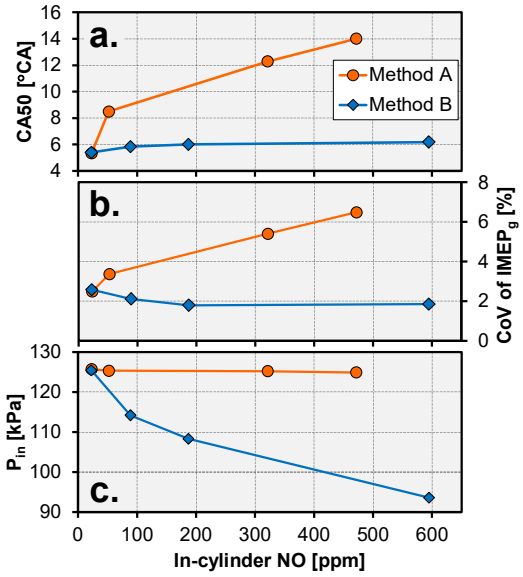

Fig. 8 Comparison of two operational techniques for studying the response of lean knock to changes of [NO]. Continuously fired operation with $\phi_{end\text{-}gas} = 0.50$ and High-Olefin fuel.

To maintain CoV of IMEP$_g$ below acceptable thresholds (ideally < 3%, and strictly < 5%), an alternative Method B was developed. In this case, P_{in} is reduced with added NO to maintain a constant KL-CA50 throughout the range of tested [NO]. With Method B, CoV of IMEP$_g$ is maintained near 2% throughout the tested range of [NO]. The autoignition-promoting effect of added NO is equally clear with Method B. Figure 8c shows that P_{in} has to be reduced strongly when NO is added. For both methods, Fig. 8 reveals that the highest sensitivity to changes of [NO] is encountered for low levels of NO. This motivates skip-fired efforts to probe the effect of changes to [NO] for levels lower than what could be achieved in these continuously fired experiments (< 25 ppm).

Skip-Fired Operation with NO-seeding

To probe the effect of changes to [NO] on the lean knock limits, a skip-fired operating scheme was adopted from Ref. [10]. It uses 4 motored cycles to purge out essentially all combustion products generated by a single fired cycle, in a repeating scheme that is illustrated in Fig. 3 of Ref. [10]. Compared to continuously fired operation, the thermal state of the engine changes when a skip-firing scheme is implemented. Before the NO-seeding sweep could be performed, three measures were taken to ensure good correspondence between the continuously fired and skip-fired data sets. First, a comparison of Tables 3 and 5 reveals that the coolant temperature was increased from 75 to 90°C. Second, Table 5 shows that for each fuel some adjustments to the baseline P_{in} and T_{in} had to be performed to achieve KL-CA50 ≈ 5°CA for an [NO] level that corresponds to that of normal continuously fired operation with KL-CA50 ≈ 5°CA. For the High-Olefin fuel, T_{in} was increased from 43 to 79°C. For the High-Cycloalkane fuel, P_{in} was increased

from 125 to 130 kPa. Also, the start of injection was retarded somewhat for the High-Cycloalkane fuel to avoid elevated soot PM emissions at these cooler skip-fired conditions. Compared to the High-Olefin fuel, Table 2 shows that the High-Cycloalkane fuel has a higher sooting propensity as indicated by its higher PMI value.

Table 5. Skip-fired operating conditions.

Engine Speed	1400 rpm	
Mode	Fire1 - Skip 4	
End-gas ϕ	0.5 (including air residuals)	
Injection Pressure	120 bar	
# of Fuel Injections	3 early + 1 pilot	
ΔCA between SOIs of Early Fuel Injections	14°CA	
Spark Energy	106 mJ	
Spark Timing Criterion	KI = 60 - 80	
Coolant Temperature	90°C	
Fuel	**High Olefin**	**High Cycloalkane**
Start of First Injection	-310°CA	-270°CA
Intake Temperature	79°C	43°C
Baseline [NO]	23 ppm	26 ppm
Baseline P_{in}	125 kPa	130 kPa

In addition, for both the baseline points and operating points with varying [NO], the pilot duration was adjusted to maintain a nearly constant dwell between ST and CA10 (*cf.* Fig. 2). With these adjustments, Fig. 9 shows that the deflagration-based AHRR has good correspondence between the two modes of operation. In this ensemble-averaged graph, the AHRR peak associated with end-gas autoignition is taller for the skip-fired operation. This is primarily a result of a more repeatable autoignition timing for the skip-fired operation. This will be discussed further in conjunction with Fig. 11.

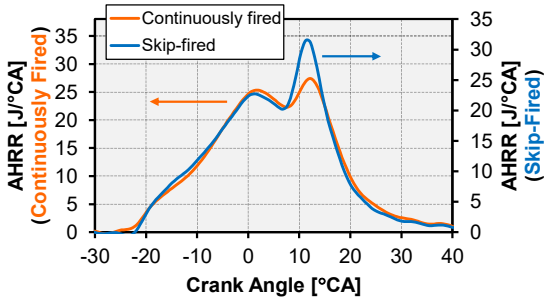

Fig. 9 Comparison of AHRR for continuously and skip-fired operation. High-olefin fuel with [NO] = 23 ppm.

Figure 10 summarizes the results from these skip-fired NO-seeding experiments. Figure 10a shows that NO plays a very important role for the knock limits of lean operation, especially for low levels of [NO]. For the current engine, trapped residuals for continuously fired operation with pilot injection results in [NO] ≈ 23 ppm. If this trapped level of [NO] could be reduced to, for instance, 1 ppm, that would increase the available $IMEP_g$ by ~16 % for either of the examined RON98 fuels. Practically, such reduction could be achieved by elimination of the pilot injection and generally improved mixture formation to minimize the amount of regions with ϕ > 0.5 [28]. Positive valve overlap with combustion-chamber scavenging using a mechanical booster is another possibility for minimizing the level of trapped NO.

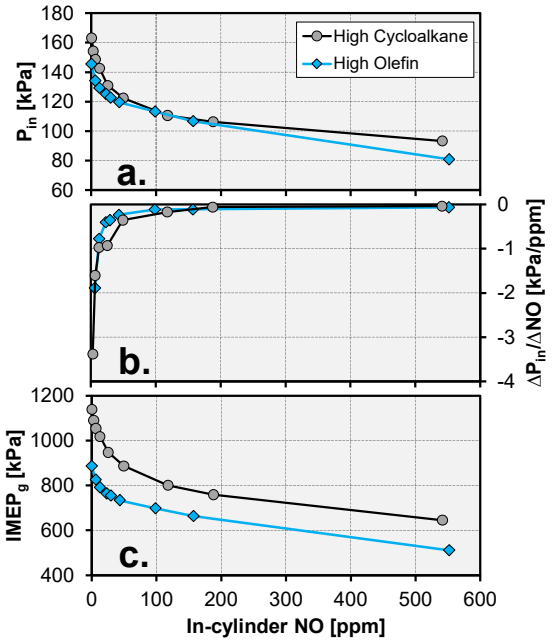

Fig. 10a) Response of knock-limited P_{in} to changes of in-cylinder [NO] for operation with CA50 = 5°CA. b) Sensitivity of P_{in} at knock limit to incremental changes of [NO], c) $IMEP_g$. Skip-fired operation with $\phi_{end\text{-}gas}$ = 0.50.

The results from continuously fired operation plotted in Fig. 7 highlight the detriment of cycle-to-cycle variability for lean SI combustion. The skip-fired results in Fig. 10 allow further insights into the sources of cycle-to-cycle variability in AHRR. Figure 11 compares the AHRR for continuously and skip-fired operation using the High-Olefin fuel. Data for both types of engine operation at an identical [NO] exist only for [NO] = 23 ppm. Here, it is clear that the skip-fired operation has substantially more consistent AHRR associated with end-gas autoignition, manifested as the peak near CA70. Consistent with this, the standard deviation of KI is lower for the skip-fired operation (35 vs. 41 kPa). It is hypothesized for the continuously fired case, cycle-to-cycle variability of the trapped [NO] contributes to elevate the variability of both end-gas autoignition and knock. Furthermore, Fig. 11 shows a smaller difference in autoignition-AHRR between the 595 and 690 ppm cases. Also, the standard deviation of KI is very similar, 38 vs. 37 kPa. The reduction of variability for the continuously fired operation at higher [NO] is consistent with the results

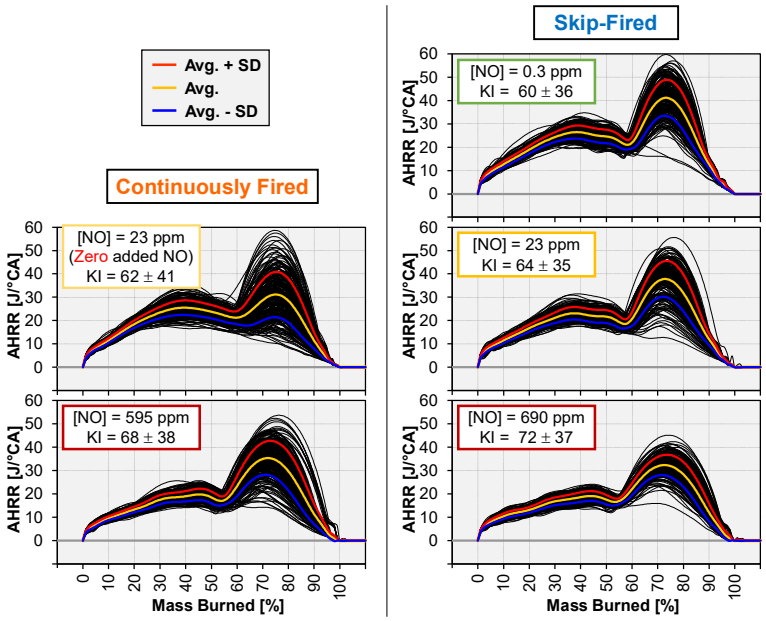

Fig. 11 Comparison of AHRR variability for lean continuously fired and lean skip-fired operation. High-Olefin fuel.

in Fig. 10b, which shows that the relative sensitivity of the knock limit decreases with increased [NO].

Lastly, the graph for skip-fired operation with 0.3 ppm NO in Fig. 11 shows reasonably repeatable AHRR, despite Fig. 10b indicating a very high sensitivity of the knock limits to small changes of [NO]. This suggest that stable knock-free operation near the lean knock limit can be achieved as long as the residual composition (and temperature) has very low cycle-to-cycle variability.

Examination of Figs. 10a and 10b reveals that the High-Cycloalkane fuel has a higher absolute sensitivity to changes of [NO] in the range of 6 to 120 ppm. The reason for this is not known, but it could be due to differences in the role of NO for both low- and intermediate-temperature autoignition reactions [10,29]. Future work is needed to clarify this.

Lastly, the results in Fig. 10a can be tied back to the observations in Fig. 5a. Figure 5a shows that the knock limit of the High-Cycloalkane fuel benefits most from the reduction of ϕ from 1.0 to 0.5, which also reduces [NO] from 116 to 33 ppm (not plotted). Based on the results in Fig. 10a, it seems likely that the higher sensitivity of the High-Cycloalkane fuel to changes of [NO] contributes to the different trends shown in Fig. 5a.

Knock Frequency Content – Stoich. and Lean

The results above highlight the importance of lean knock limits for lean SI engine operation. The benefits of shorter burn duration and higher efficiency from operating close to the knock limits are clear. At the same time, excessive engine noise is unacceptable for passenger vehicles, further emphasizing the need to control knock.

Compared to stoichiometric operation, lean SI engine operation reduces the in-cylinder charge temperatures. This lowers the speed of sound and has the potential to lower the frequency content of any in-cylinder acoustic oscillation. A shift of knock frequencies can have important implications on knock transmission to the outer surface of the engine, as well as further transmission to the driver and passenger compartment. In the following, examples will be provided of how lean combustion influences knock frequencies and associated transmission.

Figure 12a compares the in-cylinder knock content for operation with $\phi_{\text{end-gas}} = 1$ and 0.5. In this work, frequencies below 4 kHz are considered to be associated with the combustion itself rather than acoustic in-cylinder oscillations due to end-gas autoignition [11]. For $\phi_{\text{end-gas}} = 1$, a strong peak is found around 6.7 kHz. This peak corresponds to the first circumferential (1,0) oscillatory mode [30]. Furthermore, Fig. 12a shows that the lean combustion reduces the frequency of the peak corresponding to the first circumferential mode by about 13%, shifting it to near 5.9 kHz. The higher modes are also shifted to lower frequencies for the lean case, and the relative shift is slightly larger, ~20%.

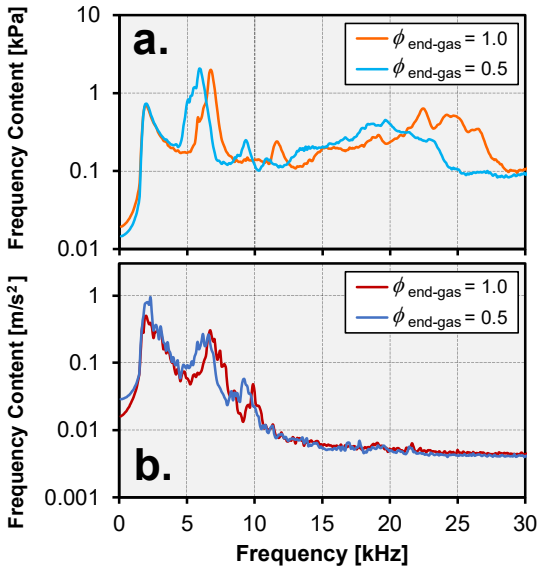

Fig. 12 Effect of stoichiometry on energy content of acoustic knock measured with the a) pressure transducer and b) accelerometer. High-Olefin fuel.

Figure 12b shows the corresponding frequency content of the surface-mounted accelerometer. The very low energy content above 10 kHz is striking, but also expected. First, it has been established that typical engine hardware strongly attenuate higher-frequency vibrations that originate from the combustion chamber [31]. Second, the accelerometer used here has a low sensitivity for the higher frequencies in the examined range. Even so,

Fig. 13b clearly shows a shift in the frequency of the peak associated with the first circumferential (1,0) mode, similar to that of the in-cylinder pressure content.

The observed frequency reduction of the in-cylinder knock oscillations can have practical implications for vehicle noise levels. The work of Shalari *et al.* [31] reveals that a generic engine structure attenuation curve has a strong reduction of the sound attenuation for decreasing frequencies in the 3 - 10 kHz range. This combined with the observations in Fig. 12a suggests that lean combustion can have a more efficient knock transmission from the combustion chamber to the outer engine surfaces, further adding importance to the topic of knock mitigation for lean-burn SI engines.

SUMMARY AND CONCLUSIONS

Ultra-lean SI engine operation has been investigated in a DISI engine using four different gasoline fuels with varying RON, S and compositions. For this low-tumble engine, it was discovered that efficient operation with $\phi_{end\text{-}gas}$ = 0.5 (λ = 2) is closely tied to the onset of acoustic knock. This happens because a combustion phasing near TDC is required to ensure sufficiently fast combustion for such ultra-lean conditions. For the conditions investigated with a CR = 12 combustion system, both a RON92-S7 and a RON100-S0 fuel were too knock limited, therefore failing to establish stable ultra-lean combustion at or near the target $IMEP_g$ of 8 bar. In contrast, the use of RON98-S10 and RON98-S11 fuels enabled stable operation for $\phi_{end\text{-}gas}$ = 0.5 conditions and revealed the following:

- For $\phi_{end\text{-}gas}$ = 1 operation, the knock-limited CA50s for the two RON98-S10/S11 fuels were essentially identical, confirming similar autoignition and knock characteristics for fuels with well-matched RON and S.
- For $\phi_{end\text{-}gas} \approx 0.5$ operation, the two fuels exhibited noticeable difference in knock resistance, suggesting that RON and S may fail to accurately rank fuels' propensity to knock under fuel-lean condition.
- Skip-fired operation and continuously fired operation were used to probe the effect of NO retained in the residuals on autoignition and knock for lean operation. For both fuels, the sensitivity to changes in NO is greatest for [NO] < 50 ppm. If single-ppm level of NO can be consistently ensured in the reactants, this can enable substantially higher engine loads before knock limits are encountered.
- Lastly, with a reduction of combustion temperatures due to the lean operation, the in-cylinder knock shifts to lower frequencies, which may promote knock transmission through the engine structure. This makes it even more important to control knock for lean operation.

Acknowledgements

The authors would like to thank Alberto Garcia, Keith Penney, Aaron Czeszynski and Tim Gilbertson for their dedicated support of the DISI laboratory. Eshan Singh and Gustav Nyrenstedt provided valuable feedback on the manuscript.

Financial support for this study was provided by Toyota Motor Corporation under agreement FI 083130924. Support for establishing the engine lab used in this study was provided by the Vehicle Technologies Office at U.S. Department of Energy (DOE), Office of Energy Efficiency and Renewable Energy (EERE). The fuels used in this study were developed as part of the Co-Optimization of Fuels & Engines (Co-Optima) project sponsored by the U.S. DOE. Sandia National Laboratories is a multi-mission laboratory managed and operated by National Technology and Engineering Solutions of Sandia, LLC., a wholly owned subsidiary of Honeywell International, Inc., for the U.S. Department of Energy's National Nuclear Security Administration under contract DE-NA0003525.

This paper describes objective technical results and analysis. Any subjective views or opinions that might be expressed in the paper do not necessarily represent the views of the U.S. Department of Energy or the United States Government.

NOMENCLATURE

AHHR: Apparent Heat-Release Rate
AKI: Anti-Knock Index
BEV: Battery-Electric Vehicle
CA: Crank Angle
CAxx: xx% Burn Point (xx = 10, 50, 70 or 90)
CR: Compression Ratio
CoV: Coefficient of Variation
FFT: Fast Fourier Transform
GHG: Greenhouse Gas Emissions
$IMEP_g$: Indicated Net Effective Pressure - gross
KI: Knock Intensity
KL: Knock Limited
MON: Motor Octane Number
NO: Nitric Oxide
OI: Octane Index
P_{in}: Intake Pressure
ppm: parts per million
RON: Research Octane Number
S: Octane Sensitivity
SD: Standard Deviation
SI: Spark Ignition
ST: Spark Timing
[NO]: Mole fraction of nitric oxide (in intake)
$[O_2]$: Mole fraction of oxygen (in intake)
ϕ: Fuel/Air-Equivalence Ratio
γ: Ratio of Specific Heats
$\eta_{th,\ gross}$: Gross Indicated Thermal Efficiency
λ: Air-Excess Ratio

REFERENCES

[1] Glasgow Climate Change Conference – October-November 2021, https://unfccc.int/

[2] Heywood, J.B., Internal Combustion Engine Fundamentals, McGraw-Hill, New York, 1988.

[3] ASTM 2699, "Research Octane Number Test." 2016, www.astm.org/Standards/D2699

[4] ASTM 2700, "Motor Octane Number Test." 2016, www.astm.org/Standards/D2700

[5] Splitter D, Pawlowski A and Wagner R (2016) A Historical Analysis of the Co-evolution of Gasoline Octane Number and Spark-Ignition Engines. Front. Mech. Eng. 1:16. doi: 10.3389/fmech.2015.00016

[6] Szybist, J.P., Busch, S., McCormick, R.L., Pihl, J.A. Splitter, D.A., Ratcliff, M., Kolodziej, C.P., Storey, J.E., Moses-Debusk, M., Vuilleumier, D., Sjöberg, M., Sluder, C.S., Rockstroh, T., and Miles, P., "What Fuel Properties Enable Higher Thermal Efficiency in Spark-Ignited Engines?", Progress in Energy and Combustion Science 82, 2021, https://doi.org/10.1016/j.pecs.2020.100876

[7] Vuilleumier D. and Sjöberg, M., "The Use of Transient Operation to Evaluate Fuel Effects on Knock Limits Well Beyond RON Conditions in Spark-Ignition Engines", SAE paper 2017-01-2234.

[8] Vuilleumier, D. Huan, X. Casey T. and Sjöberg M., "Uncertainty Assessment of Octane Index Framework for Stoichiometric Knock Limits of Co-Optima Gasoline Fuel Blends", SAE International Journal of Fuels and Lubricants 11(3):247–269, 2018, https://doi.org/10.4271/04-11-03-0014

[9] Sjöberg, M., Zeng, W., Singleton, D., Sanders, J. *et al.*, "Combined Effects of Multi-Pulse Transient Plasma Ignition and Intake Heating on Lean Limits of Well-Mixed E85 DISI Engine Operation," SAE Int. J. Engines 7(4):1781-1801, 2014,: https://doi.org/10.4271/2014-01-2615

[10] Sjöberg, M., Vuilleumier, D., Kim, N., Yokoo, N., Tomoda T., and Nakata K., "On the Role of Nitric Oxide for the Knock-Mitigation Effectiveness of EGR in a DISI Engine Operated with Various Gasoline Fuels", JSAE/SAE Technical Paper 20199084/2019-01-2150, 2019.

[11] Sjöberg, M., Vuilleumier, D., Yokoo N., and Nakata K., "Effects of Gasoline Composition and Octane Sensitivity on the Response of DISI Engine Knock to Variations of Fuel-Air Equivalence Ratio", COMODIA 2017, July 25 – 28, Okayama, Japan.

[12] Tornatore C. and Sjöberg M., "Optical Investigation of a Partial Fuel Stratification Strategy to Stabilize Overall Lean Operation of a DISI Engine Fueled with Gasoline and E30", Energies, 2021; 14(2):396.

[13] Fouts, L., Fioroni, G.M., Christensen, E., Ratcliff, M. et al., "Properties of co-optima core research gasolines," Report No. NREL/TP-5400-71341, Golden, CO: National Renewable Energy Laboratory, 2018.

[14] Kalghatgi, G., "Fuel Anti-Knock Quality - Part I. Engine Studies," SAE Technical Paper 2001-01-3584, 2001, https://doi.org/10.4271/2001-01-3584

[15] Mittal, V. and Heywood, J., "The Relevance of Fuel RON and MON to Knock Onset in Modern SI Engines," SAE Technical Paper 2008-01-2414, 2008, https://doi.org/10.4271/2008-01-2414

[16] Ayala F., Gerty, M., Heywood J., "Effects of Combustion Phasing, Relative Air-fuel Ratio, Compression Ratio, and Load on SI Engine Efficiency", SAE Technical Paper 2006-01-0229, 2006, https://doi.org/10.4271/2006-01-0229

[17] Sjöberg, M. and He, X., "Combined effects of intake flow and spark-plug location on flame development, combustion stability and end-gas autoignition for lean spark-ignition engine operation using E30 fuel", International Journal of Engine Research, Vol 19, Issue 1, pp. 86 – 95, January 2018, doi: 10.1177/1468087417740290

[18] Takahashi, D., Nakata, K., Yoshihara, Y., and Omura, T., "Combustion Development to Realize High Thermal Efficiency Engines," SAE Int. J. Engines 9(3):2016, doi:10.4271/2016-01-0693

[19] Kaneko, K., Yasutake, Y., Yokomori, T., and Iida, N., "Influence of ethanol blending on knocking in a lean burn SI engine," SAE Technical Paper 2019-01-2152, 2019, doi: 10.4271/2019-01-2152

[20] Waqas, M.U., Hoth, A., Gainey, B., Johansson, B. et al., "Effect of Intake Temperature and Engine Speed on the Auto-Ignition Reactivity of the Fuels for HCCI Fuel Rating," SAE Technical Paper 2021-01-0510, 2021, doi:10.4271/2021-01-0510

[21] Lopez-Pintor, D. and Dec, J.E., "Experimental Evaluation of a Gasoline-like Fuel Blend with High Renewable Content to Simultaneously Increase φ-Sensitivity, RON, and Octane Sensitivity", Energy & Fuels 35(20) 2021, https://doi.org/10.1021/acs.energyfuels.1c01979

[22] Silke, E., Pitz, W., Westbrook, C., Sjöberg, M. et al., "Understanding the Chemical Effects of Increased Boost Pressure under HCCI Conditions," SAE Int. J. Fuels Lubr. 1(1):12-25, 2009, https://doi.org/10.4271/2008-01-0019

[23] Leone, T., Olin, E., Anderson, J., Jung, H. et al., "Effects of Fuel Octane Rating and Ethanol Content on Knock, Fuel Economy, and CO2 for a Turbocharged DI Engine," SAE Int. J. Fuels Lubr. 7(1):2014, doi:10.4271/2014-01-1228

[24] Naiki, T., Obata, K., Watanabe, M., Yokomori, T., Iida, N., "Research of Fuel Components to Expand Lean-limit in Super Lean-burn Condition", JSAE / SAE Technical Paper 20199306 / 2019-01-2257.

[25] T. Yokomori, N. Iida, et al., "Research on Super Lean Burn Concept for Gasoline Engine with High Thermal Efficiency", JSAE 20165267, 2016.

[26] Mahendar, S., Giramondi, N., Venkataraman, V., and Christiansen Erlandsson, A., "Numerical Investigation of Increasing Turbulence through Piston Geometries on Knock Reduction in Heavy Duty Spark Ignition Engines," SAE Technical Paper 2019-01-2302, doi: 10.4271/2019-01-2302

[27] Roberts, P. and Sheppard, C., "The Influence of Residual Gas NO Content on Knock Onset of Iso-Octane, PRF, TRF and ULG Mixtures in SI Engines," SAE Int. J. Engines 6(4):2028-2043, 2013, doi: 10.4271/2013-01-9046.

[28] Steeper, R.R. and De Zilwa, S., "Improving the NO_x-CO_2 Trade-Off of an HCCI Engine Using a Multi-Hole Injector", SAE Technical Paper 2007-01-0180, 2007.

[29] Fang, R., Saggese, C., Wagnon, S.W., Sahu, A.B., Curran, H.J., Pitz, W.J. and Sung C.-J., "Effect of nitric oxide and exhaust gases on gasoline surrogate autoignition: iso-octane experiments and modeling", Combustion and Flame 236, 2022.

[30] Draper, C.S., "Pressure Waves Accompanying Detonation in the Internal Combustion Engine", Journal of Aeronautical Sciences 5(6), 1938, https://doi.org/10.2514/8.590

[31] Shahlari A.J., Hocking C., Kurtz E. and Ghandhi J., "Comparison of Compression Ignition Engine Noise Metrics in Low-Temperature Combustion Regimes", SAE Int. J. Engines 6(1):2013, https://doi.org/10.4271/2013-01-1659